

PAPER • OPEN ACCESS

EXAFS investigations on the pressure induced local structural changes of GeSe₂ glass under different hydrostatic conditions




To cite this article: Emin Mijit *et al* 2023 *J. Phys.: Condens. Matter* **35** 264001

View the [article online](#) for updates and enhancements.

You may also like

- [Investigational study on Influence of Fiber Reinforced Polymer Wrapping on Concentrically Loaded Concrete Column](#)
N Pannirselvam, B SudalaiGunaseelan and J Rajprasad
- [Damage behavior analysis of smart composites with embedded pre-strained SMA foils](#)
Toshimichi Ogisu, Masakazu Shimanuki, Satoshi Kiyoshima *et al.*
- [XAS studies of pressure-induced structural and electronic transformations in -FeOOH](#)
N Trcera, S Layek, M Shulman *et al.*

EXAFS investigations on the pressure induced local structural changes of GeSe₂ glass under different hydrostatic conditions

Emin Mijit^{1,*} , João Elias F S Rodrigues² , Georghii Tchoudinov¹,
Francesco Paparoni¹ , Toru Shinmei³, Tetsuo Irfune³, Olivier Mathon²,
Angelika Dorothea Rosa² and Andrea Di Cicco^{1,*}

¹ Physics Division, School of Science and Technology, Università di Camerino, Via Madonna delle Carceri 9, I-62032 Camerino, (MC), Italy

² European Synchrotron Radiation Facility, 71, Avenue des Martyrs, CS 40220, 38043 Grenoble, Cedex 9, France

³ Geodynamics Research Center, Ehime University, Matsuyama 790–8577, Japan

E-mail: emin.mijiti@unicam.it and andrea.dicicco@unicam.it

Received 3 January 2023, revised 16 March 2023

Accepted for publication 28 March 2023

Published 6 April 2023



CrossMark

Abstract

Pressure-induced transformations in glassy GeSe₂ have been studied using the x-ray absorption spectroscopy. Experiments have been carried out at the scanning-energy beamline BM23 (European Synchrotron Radiation Facility) providing a micrometric x-ray focal spot up to pressures of about 45 GPa in a diamond anvil cell. Both Se and Ge K-edge experiments were performed under different hydrostatic conditions identifying the metallization onsets by accurate determinations of the edge shifts. The semiconductor-metal transition was observed to be completed around 20 GPa when neon was used as a pressure transmitting medium (PTM), while this transition was slightly shifted to lower pressures when no PTM was used. Accurate double-edge extended x-ray absorption fine structure (EXAFS) refinements were carried out using advanced data-analysis methods. EXAFS data-analysis confirmed the trend shown by the edge shifts for this disordered material, showing that the transition from tetrahedral to octahedral coordination for Ge sites is not fully achieved at 45 GPa. Results of present high pressure EXAFS experiments have shown the absence of significant neon incorporation into the glass within the pressure range up to 45 GPa.

Keywords: high pressure, polyamorphism, glasses, x-ray absorption spectroscopy

(Some figures may appear in colour only in the online journal)

* Authors to whom any correspondence should be addressed.



Original Content from this work may be used under the terms of the [Creative Commons Attribution 4.0 licence](https://creativecommons.org/licenses/by/4.0/). Any further distribution of this work must maintain attribution to the author(s) and the title of the work, journal citation and DOI.

1. Introduction

The behavior of amorphous–amorphous transformations (polyamorphism) has been investigated over the years, mostly in covalently bonded systems with open local structures, such as amorphous forms of Si, Ge, SiO₂, GeO₂ and ice [1–5]. Among these systems, amorphous SiO₂ has been the most popular subject for studies of pressure induced polyamorphism in network forming glasses, as a simple analogue to the silicate melts which are one of the major components in the Earth and other planetary interiors. Pressure-induced changes in the short and intermediate range structural ordering in simple network forming glasses have been extensively studied in the last few decades by means of various experimental techniques such as x-ray diffraction (XRD), x-ray absorption, Raman and Brillouin spectroscopy [1–12]. It is well established now that the low density amorphous (LDA) to high density amorphous (HDA) transformations in these glasses are closely associated with some important changes in the local and intermediate structures, such as the gradual increase of nearest neighbor coordination numbers (CNs) (typically from 4 to 6) and collapse of voids and empty interstitial spaces [1, 3, 4, 6–12].

Moreover, structure of amorphous SiO₂ and other geophysical relevant glasses have been studied under high pressure together with noble gases in order to verify the possible storage and solubility of noble gases in silicate or other oxide melts [8, 10, 13–19]. On the other hand, noble gases are widely used as hydrostatic pressure-transmitting mediums (PTMs) for high pressure experiments with diamond anvil cells (DACs) [20], thus the effect of noble gas PTMs on the pressure response of glassy systems needs to be clarified. Indeed, previous experiments have shown that helium (He) can easily penetrate into the structure of silica glass and strongly alter its compressibility and rigidity [8, 10, 18]. Experiments on basalt and enstatite glasses also indicated the incorporation of neon (Ne) into the glass structure under high pressure [15].

In the context of high-pressure investigation of glasses, the x-ray absorption spectroscopy (XAS) represents a powerful element selective probe to identify local structural changes under extreme conditions (see for example [21] and references therein). High pressure XAS investigations about glass polyamorphism are generally performed on systems of mid-Z elements (being Z the atomic number), such as amorphous Ge [2, 7], GeO₂ [4, 22], and NaAlGe₃O₈ as a structural analog to SiO₂ and other structurally complex silicate glasses [23, 24] as well as chalcogenides [11, 12]. Compatibility of these systems with high pressure XAS experiments provides a unique opportunity for element-specific studies of pressure-induced electronic and structural changes in glassy systems. XAS spectroscopy provides accurate local structural information and can be used to investigate possible effects introduced by the incorporation of noble gases and other minor trace elements into the disordered systems (see for example [25, 26]). Nowadays, high pressure extended x-ray absorption fine structure (EXAFS) experiments associated with DACs are often performed using nano-polycrystalline diamond (NPD) anvils [27, 28] to avoid spurious glitches that can be introduced by the

Bragg reflections from the single crystal diamond anvils. However, because of the easy diffusion of He into the NPD anvils, Ne is so far the best PTM of choice for high pressure EXAFS experiments performed with NPD anvils although possible side effects due to its diffusion into the glassy materials of mid-Z elements have never been reported.

In this work, we present a new Ge and Se K-edge XAS study on the pressure behavior of glassy GeSe₂ (g-GeSe₂) up to ~45 GPa under different experimental conditions (with and without Ne PTM). The main building blocks of the network in these glasses are the covalently bonded GeSe₄ tetrahedra, which are connected either by edge or corners, as in case of its ambient pressure crystalline phase (see figure 1). This particular composition of the Ge-Se chalcogenide glass systems has been studied previously under high pressure by means of first principle molecular dynamics (up to 80 GPa) [29], x-ray and neutron diffraction (up to 16 GPa) [30, 31], and acoustic measurements (up to 9.6 GPa) [32]. Experimental investigations on the properties of g-GeSe₂ above 16 GPa were performed so far only by our group using XAS measurements up to 30 GPa [33]. In that previous study, high pressure XAS data have been collected using dispersive geometry (at the ODE beamline of Synchrotron SOLEIL), so with limited useful EXAFS range and signal to noise ratio as compared to standard scanning energy beamlines. Analysis of those dispersive XAS data have shown two compression stages, first decrease of the first neighbor Ge-Se distances up to 10 GPa then a subsequent increase of the Ge-Se distances, bond disorder and CNs [11]. However, the expected gradual conversion from tetrahedral to octahedral configuration (suggested by MD simulations in [29]) was not completed at 30 GPa. For this work, we performed our experiments at the BM23 scanning-energy beamline at the ESRF (European Synchrotron Radiation Facility) exploiting its micrometer focusing capabilities for high-pressure experiments with DACs. The new high-quality data allowed us to perform a careful EXAFS double-edge analysis with the aim of measuring the evolution of the local structure beyond the previously investigated pressure ranges. We also compared the pressure behavior of the g-GeSe₂ under different experimental conditions, in order to assess the possible side effects of the Ne PTM on the local structure of g-GeSe₂ under high pressures.

2. Experiments

Fine powders of g-GeSe₂ samples have been purchased from Sigma-Aldrich (CAS number 12065-11-1, 99.999% purity). High pressure EXAFS experiments on g-GeSe₂ have been performed using a membrane DAC equipped with NPD anvils [27, 28] to obtain glitch-free EXAFS spectra. Two compression runs (with and without PTM) have been performed. For the first compression run, NPD anvils with 300 μm culet size were used. A rhenium gasket with 200 μm initial thickness was pre-indented to a final thickness of ~45 μm and laser drilled to obtain a sample chamber of about ~170 μm diameter. A small piece of a uniform g-GeSe₂ pellet (with lateral dimension of about ~50 μm and thickness of about ~25 μm, made by compressing the fine powders) has been placed at the center

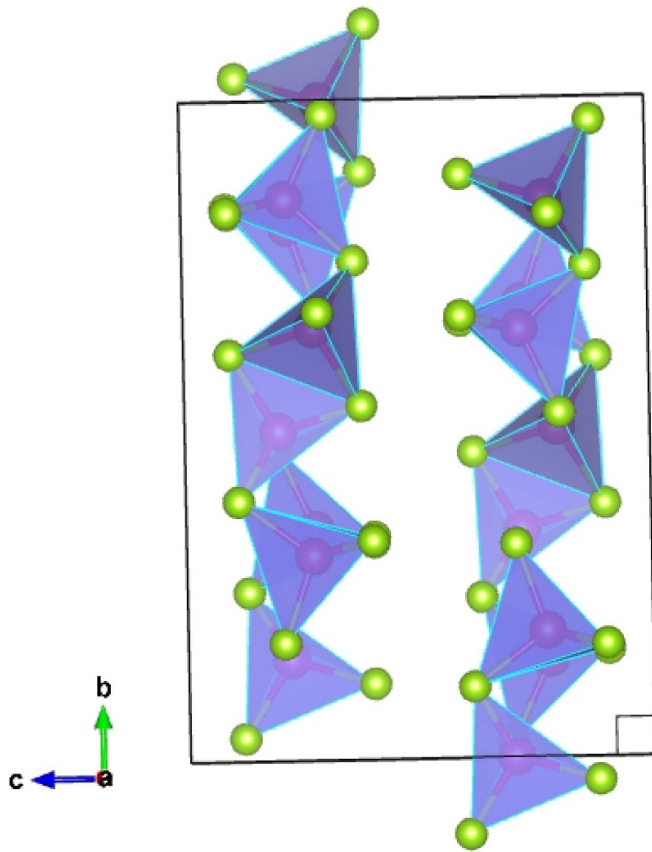


Figure 1. Structure of the ambient pressure crystalline phase (monoclinic, spacegroup: $P21/c$) of GeSe_2 . Red and green balls represent Ge and Se atoms, respectively.

of the sample chamber together with a tiny piece of gold (Au). The sample chamber was then filled with Ne as PTM. For the second run, NPD anvils with $150\ \mu\text{m}$ culet size were used. A $200\ \mu\text{m}$ thick rhenium gasket was pre-indented to a final thickness of $\sim 30\ \mu\text{m}$ and laser drilled to obtain a sample chamber of about $\sim 75\ \mu\text{m}$ diameter. The sample chamber was filled entirely with amorphous GeSe_2 powders, without any PTM but with a small piece of gold (Au). Pressures were measured using the equation of state of Au [34]. Pressure measurements using standard ruby fluorescence technique have been avoided during the entire experimental procedures for preventing the possible laser induced crystallization of the GeSe_2 glass. Before each measurement, pressure was stabilized for about 10 min.

After the sample loading into the DAC, EXAFS data have been measured at room temperature under increasing static pressures up to 45 GPa at the BM23 beamline of the European Synchrotron Radiation Facility (ESRF, France) [35]. A double crystal monochromator equipped with two Si(111) crystals in fixed exit geometry was employed for monochromatizing the incoming beam. The x-ray beam was focused down to $3 \times 3\ \mu\text{m}^2$ using two Pt coated mirrors inclined to 4.0 mrad in Kirkpatrick–Baez (KB) geometry that served also for harmonic rejection. EXAFS data have been measured in transmission mode (in axial geometry through the diamond anvils) scanning through both Ge and Se K-edges at each pressure

point. Reference spectra of a g- GeSe_2 pellet at ambient conditions have been also simultaneously measured for each XAFS data for the purpose of edge energy calibration. XRD patterns have also been collected for measuring the pressure from the Au calibrant, but also to monitor sample status (amorphous or crystal) at selected pressures. XRD measurements were performed using a Pilatus 1 M detector by fixing the monochromator energy at 18.0 keV ($0.6888\ \text{\AA}$). The sample to detector distance, detector tilt and incident beam position were calibrated using a cerium oxide powder standard. No sign of crystallization has been evidenced during our compression runs.

3. Results

Traditionally, the XAS spectrum is divided into two regions. The structure in the vicinity of the edge is referred to as x-ray absorption near-edge structure (XANES). While the oscillations above the edge, which can extend for several hundred eV or more, are often referred to as EXAFS. These two sections of the XAS spectra have different degrees of sensitivity to the short and medium range structural ordering and are complementary to each other. We will present and analyze the high pressure XAS data sets step by step, starting with the XANES section which will be followed by the quantitative analysis of EXAFS signals in the subsequent sections.

3.1. XANES analysis

Ge and Se K-edge XANES spectra measured along two compression runs (with and without PTM) are compared for selected pressure points in figures 2(a) and (b), respectively. We can see that XANES spectra of both edges show clear changes under high pressure. In both Ge and Se K-edges, features above the white line peak (indicated by vertical arrows) become broadened and gradually disappear at about 28 GPa in substantial agreement with the trend previously observed in [11]. Because of the larger mean free path of the low energy photo-electrons and relevance of higher order many body multiple scattering signals, XANES features are known to be sensitive to the pressure induced modifications in the 3D atomic configurations beyond the nearest coordination shell [36–43]. Therefore, such changes in the XANES spectra reflect the occurrence of modifications in the short and intermediate range structural ordering of the glass network along the gradual LDA-HDA transformation which takes place in the 10–30 GPa pressure range (see the next sections). As shown in figure 2(b), Se K-edge XANES measured with and without PTM (Ne) are nearly identical in this pressure range. At the Ge K as well, XANES data of initial (4.0–4.7 GPa) and final (44–46 GPa) pressure points are very similar for the two different experimental conditions, while there are minor spectral differences at intermediate pressures (around 18 and 28 GPa). Similarity of the Ge K-edge data at the initial and final pressure points indicate that the short and intermediate range structural ordering in LDA and HDA forms of g- GeSe_2 glass are the same for both experimental conditions (with and without Ne PTM), suggesting

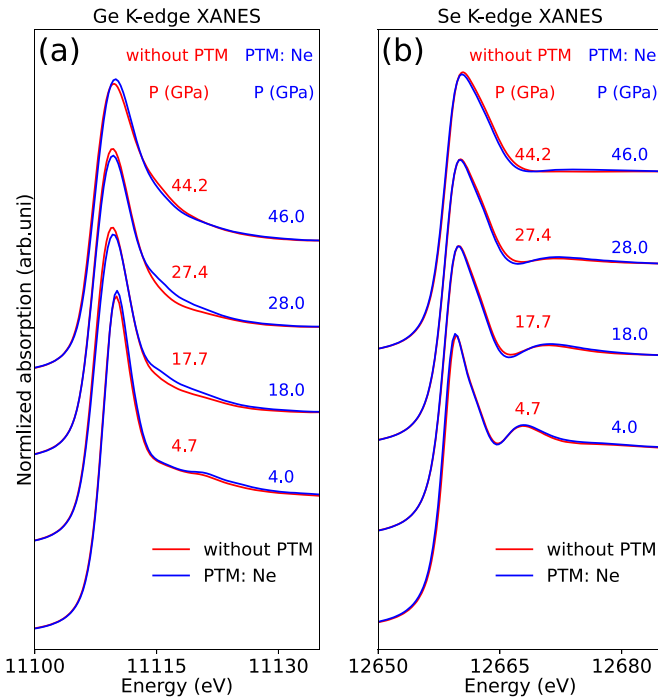


Figure 2. Comparison of XANES spectra measured with (blue lines) and without PTM (red lines) at few selected pressure points. (a) Ge K-edge XANES. (b) Se K-edge XANES. Minor energy shifts of the edge energy (see figure 3) in the individual spectra are aligned for better comparing the spectra line shapes.

the absence of observable amount of Ne in the glass structure. Minor differences in the Ge K-edge XANES at intermediate pressures (18 and 28 GPa) are possibly due to small variations in the effective pressure for the two cases, since those are the rapidly evolving spectral features in that pressure range. The observed negligible spectral differences at the Se K-edge also excludes the presence of significant amounts of Ne in g-GeSe₂ glass within the investigated pressure ranges.

The pressure dependencies of the edge energy shift (ΔE_e) at Ge and Se K-edges have been evaluated for both experimental runs and compared in figure 3. Here, the edge energy (E_e) is defined as usual, as the energy position of the first maximum in the first derivative of the corresponding XANES spectra. As we can see in figure 3, Ge K-edge E_e exhibits a clear shift towards lower energies upon pressurization, while the Se K-edge E_e is constant within the estimated error bars in the whole pressure range, in substantial agreement with what was observed by Properzi *et al* in a previous study [11]. The energy red-shift of the Ge K-edge is rather gradual in the 10–20 GPa range, reaching typical 1.3–1.5 eV values above 30 GPa. This does not suggest a change in the oxidation state of Ge, but rather reflects the gradual gap closure and eventual metallization process above 10–15 GPa which was also predicted by theoretical calculations in [29]. Behavior of the edge energies suggest that the projected density of delocalized states near the Fermi energy has a significant overlap at the Ge sites

following the metallization accompanying the LDA to HDA transformation.

The pressure dependencies of the edge energies follow similar trends along both compression runs with and without Ne PTM, suggesting the absence of significant effect from the presence of a PTM. The measured different XANES spectral line shapes at the initial and final pressure points and the extent of the edge energy shift of the Ge K-edge (corresponding roughly to the energy gap in semiconducting g-GeSe₂) are the clear manifestation of the existence of distinct polyamorphic states in g-GeSe₂, namely the semi-conducting LDA and metallic HDA amorphous phases.

3.2. EXAFS analysis

EXAFS signals are extremely sensitive to the local atomic structure and have been widely used as a powerful probe for studying the short range structure of disordered systems (glasses and liquids, see for example [21, 44]). Thanks to the application of NPD anvils and the highly stable scanning energy setup of the BM23 beamline, extracted EXAFS signals were of good quality, allowing us to perform reliable structural refinements. Experimental EXAFS signals were analyzed using standard procedures based on *ab initio* calculations of the x-ray absorption cross-section within the framework of the GNXAS method [45–47]. Taking advantage of the advanced multi-edge refinement features of the GNXAS package [48], Ge and Se K-edge EXAFS spectra of each pressure point have been simultaneously analyzed by including a single Ge-Se coordination shell in the model. Fitting parameters such as mean atomic distances (R) and variance (σ^2) were obviously constrained to be the same for both edges. Energy shift (E_0) was floated in a narrow range (since edge energies can shift with pressure), but fixing a lower limit for it to be above the edge energy. S_0^2 is a quantity which takes into account many factors, it may also change depending on the changes in the sample (e.g. thickness, density etc). Thus, parameter S_0^2 was also floated in a very narrow range (± 0.01) around the value which was obtained with the highest quality data at the ambient pressure. The CN of the Se was fixed to be half of the CN of Ge, according to the known stoichiometry.

Several anomalous features in the EXAFS signal background which originate from multi-electron excitations and imperfect absorption compensations at the platinum (coating of the KB mirrors) L-edges (where the incoming photon flux decrease sharply) have been identified, and accounted for within the standard GNXAS refinement procedure using model functions [47].

An exemplary double-edge EXAFS refinement on a pair of Ge and Se K-edge EXAFS signals measured at 15.2 GPa is displayed in figure 4. As one can see, a good agreement between the experimental and best-fit calculated signals is achieved, demonstrating that reliable quantitative information about the first-neighbor distance distribution can be obtained from our high pressure EXAFS data. The best-fit signal here was obtained using a Gaussian first neighbor distribution

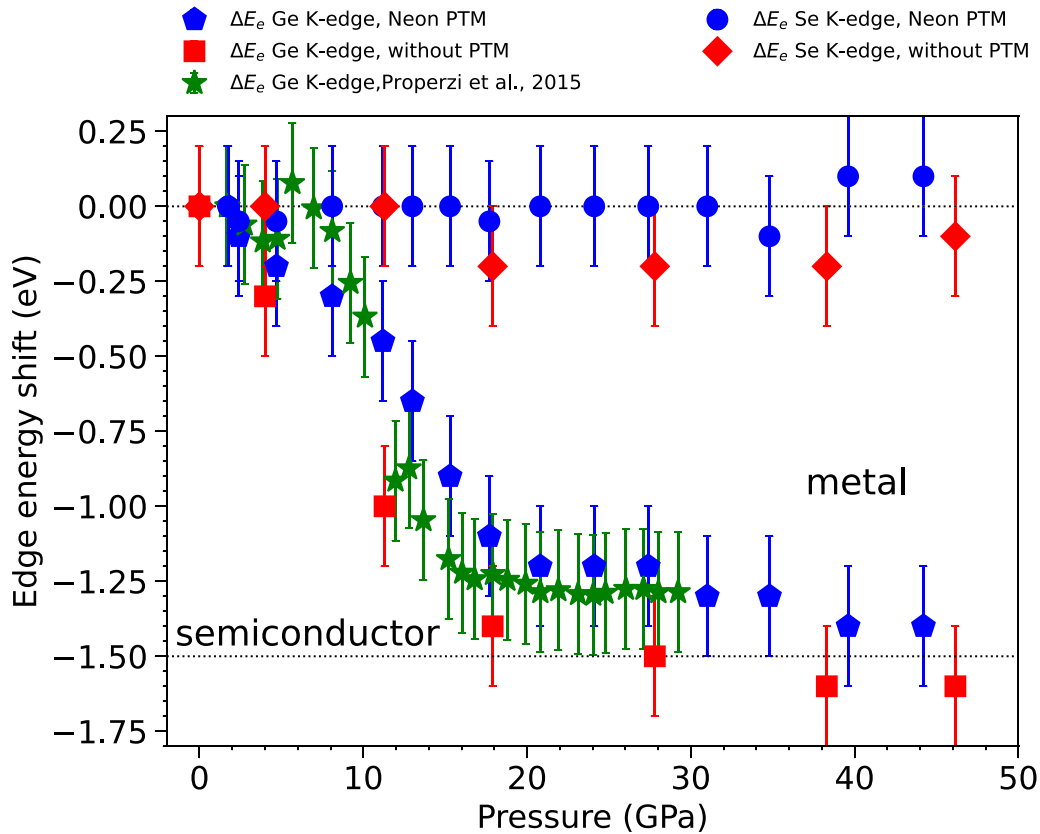


Figure 3. Shift of Ge and Se K-edge energies as a function of pressure measured in this work is compared with the Ge K-edge data of a previous work [11] (green stars in figure). The pressure dependence of the edge energy shift $\Delta E_c(P) = E_c(P) - E_c(P_0)$ was evaluated with respect to the Ge and Se K-edge energies at the ambient pressure (P_0). Data are reported for different pressure transmitting media (PTM) at Ge K-edge (square and pentagons) and Se K-edge (diamonds and circles). Experiments without PTM are reported in red color while those using Ne as a PTM in blue. Previous data (green color) of Properzi *et al* were collected using silicon oil as PTM [11].

function determined by three parameters, the average Ge–Se distance R_{GeSe} , the distance variance σ_{GeSe}^2 and the CN. The residual signals are mainly assigned to the weak contributions of the chemical disorder (Ge–Ge and Se–Se ‘wrong’ bonds) which is known to be present in g-GeSe₂ [11]. Minor contributions increasing the residual are also assigned to slightly imperfect background modelling and to farther distance correlations in the 3–4 Å region. More detailed EXAFS analysis including also the contributions due to chemical disorder are currently in progress using the relatively higher quality datasets measured along the compression run without PTM and will be reported elsewhere.

Above mentioned refinement procedures were applied for the rest of the high pressure EXAFS data, achieving satisfactory agreements between the experiment and best-fit calculated signals, as one can see from the Fourier transforms reported in figure 5. Note that Fourier transforms shown in figure 5 are mostly to demonstrate the goodness of the refinements, are not necessarily instructive of the structure. (intensities and width of the peaks in the Fourier transform depends on several factors, such as the structural disorder, noise, interference of the individual signals in the original EXAFS data). After the refinements, reliable estimates for the structural parameters R_{GeSe} , σ_{GeSe}^2 and CN were obtained, as reported in figure 6.

4. Discussion

Now we start discussing the results of the EXAFS data-analysis. As we can see from in figure 6, evolution of the structural parameters suggest the existence of three distinct stages along the compression process: (i) a first stage in the 0–~11 GPa range in which the LDA local structure is compressed but retained; (ii) a second transitional stage in the 11–~30 GPa range in which a transformation from LDA to HDA phase takes place; (iii) a third stage (30–~45 GPa) limited by the present maximal pressure in which we observed the stabilization of the HDA phase and further compression.

In particular, we have found that at the initial compression stage up to ~11 GPa, the CNs of the first neighbor Ge–Se distribution are stable around 4, while the Ge–Se average distance R_{GeSe} shows a clear decrease for increasing pressures. Slight shortening of R_{GeSe} in this initial compression stage is a consequence of maintaining a local tetrahedral ordering (around Ge atoms) while changes are expected at intermediate distances like the compaction of the empty voids and inter-layer spacing in the glass. This process is anyway accompanied by a slight increase of the disorder, as indicated by the slight rise of σ_{GeSe}^2 as shown in figure 6(a).

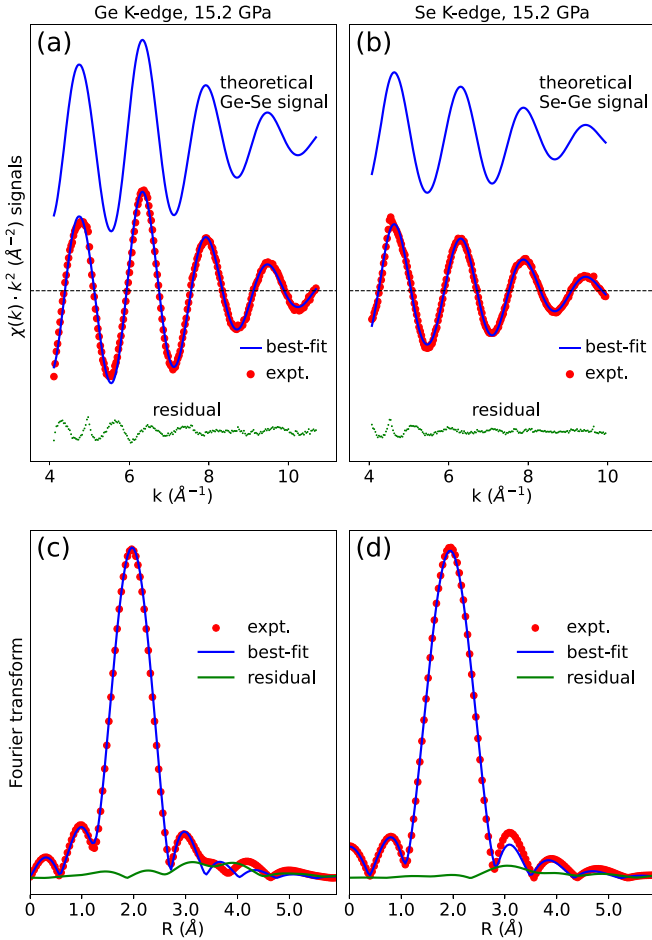


Figure 4. Exemplary double-edge refinement for the pair of Ge (a) and Se (b) K-edge EXAFS data measured at 15.2 GPa (data is from the compression run with Ne PTM). Fourier transforms of experimental and best-fit theoretical signals at the Ge and Se K-edges were shown in panel (c) and (d), respectively.

Within the 11–30 GPa range (second stage), the average distance R_{GeSe} is observed to elongate rapidly. Such a behavior is usually regarded as an important signature of LDA to HDA transformation process accompanied by the rapid increase of CNs [2, 7, 23, 49], due to the fact that the average distance needs to be larger to accommodate more atoms within the first-shell of neighbors. Indeed, we have allowed changes of CNs and best-fit results are reported in figure 6(c) also showing a rapid increase within this pressure range. As can be expected, σ_{GeSe}^2 also increased simultaneously, reflecting the drastic increase of the disorder resulting from the breakdown of a more symmetric fourfold tetrahedral coordination into a distorted local configurations characterized by an inhomogeneous penetration of the second neighbor atoms into the first shell.

In the 30–45 GPa pressure range (third stage), the average distance R_{GeSe} is observed to decrease slowly for increasing pressures, while CNs and σ_{GeSe}^2 are found to be almost stable around their maximum values, within the estimated error bars. Interestingly, average CNs above 30 GPa is around 5 instead of the expected value of 6 for a fully octahedral configuration

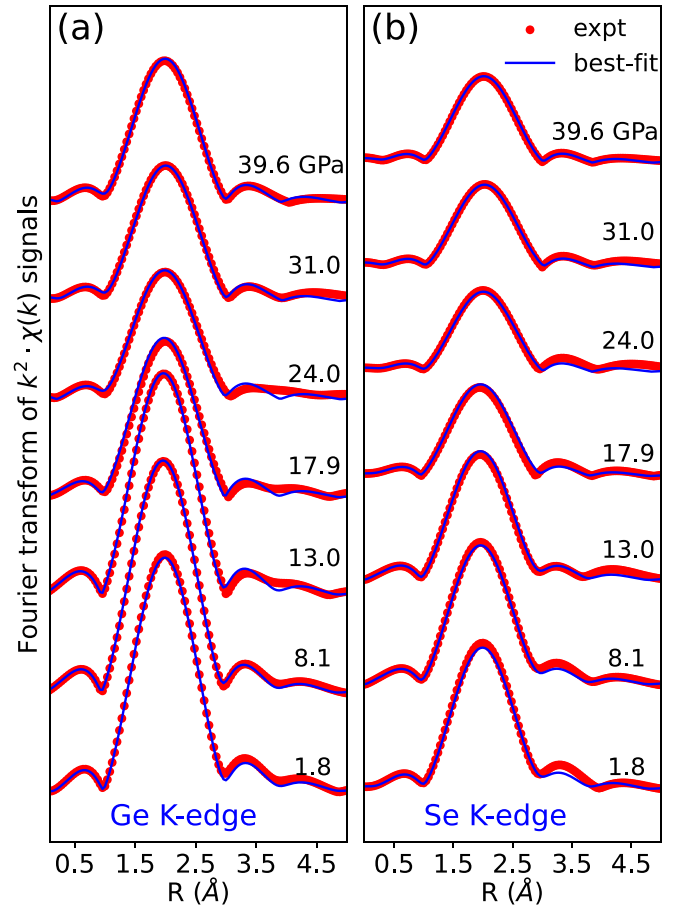


Figure 5. Fourier transforms (k -range 4.2–9.6 \AA^{-1}) of the experimental (red dots) and best-fit calculated (blue lines) EXAFS signals at selected pressures (data are from the compression run with Ne PTM). (a) Fourier transforms at the Ge K-edge. (b) Fourier transforms at the Se K-edge.

at high pressures. This suggests that the glass structure in this stage is composed of a mixture of 4, 5 and 6 fold coordinated units. Nevertheless, saturation of σ_{GeSe}^2 and gradual decrease of the atomic distance R_{GeSe} indicates the dominance of HDA component in the glass.

The results obtained by EXAFS data-analysis are accompanied by similar trends of the Ge and Se K-edge energy shown in figure 3, in which the LDA-HDA transition is clearly associated with a ~ 1.5 eV red-shift of the Ge K-edge. This value roughly corresponds to the semiconductor energy gap in this material which is obviously absent in a metal, so confirm the semiconductor-metal transition in this glass. On the other hand, the observation of a stable Se K-edge energy requires deeper investigations that will be discussed elsewhere.

As we can see in figure 6, pressure induced changes of local structural parameters (CN, R_{GeSe} and σ_{GeSe}^2) have similar trends along the two compression runs (with or without PTM) and are in qualitative agreement with previous results obtained using silicon oil as PTM [11]. The only visible effect, especially in the trend of the R_{GeSe} distances, is a slight pressure shift in the onset of the LDA-HDA transformation occurring in the 10–20 GPa range between compression runs using Ne as

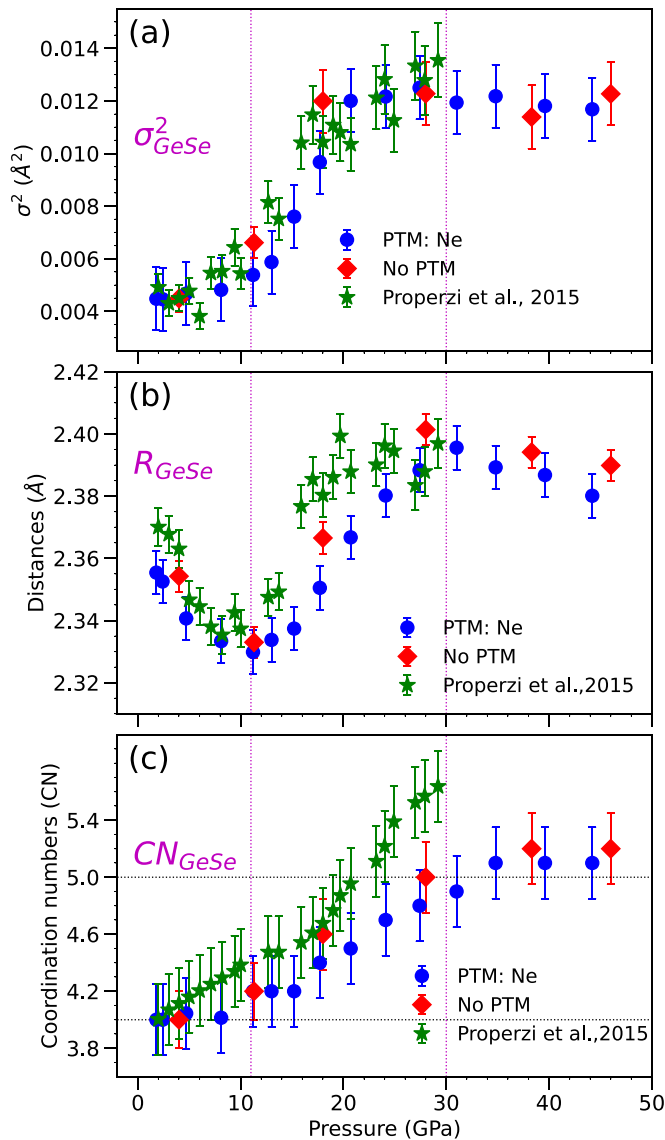


Figure 6. Best-fit structural parameters obtained by EXAFS data-analysis as a function of pressure related to the first-neighbor distribution: σ_{GeSe}^2 (a), R_{GeSe} (b), and CN (c). Refined structural parameters obtained in the present work without (red points, diamonds) or with Ne (blue points, circles) as pressure transmitting medium (PTM) are also compared to those reported by Properzi *et al* in [11] (green points, stars).

PTM and those with no PTM. A similar effect is also present in the shift of Ge K-edge shown in figure 3. Such a difference could be mainly assigned to systematic errors in the pressure measurements affecting especially those without PTM or with silicon oil where non-hydrostaticity is significant. In fact, for the compression run without PTM, the x-ray beam for EXAFS measurements was always aligned to the center of the sample chamber, but the pressure marker (tiny Au piece) was placed at one side of the sample chamber. In such non-hydrostatic conditions, it is very likely that measured pressures are systematically lower than those obtained using Ne as a PTM (variations up to 10% are quite normal). Considering those systematic errors of pressure measurements, the actual differences

(among different runs) in the evolution of relevant quantities as a function of pressure can be assumed to be negligible. The same arguments can be used also for comparing present R_{GeSe} and CN results with those reported by Properzi *et al* [11] using silicon oil as PTM, with the additional point that larger errors in the refinements (especially on CN values) can be assigned to the lower k -range and higher noise level typical of XAFS data collected in dispersive geometry.

Generally speaking, the trend of the structural parameters observed in the present work is in agreement with those in [11], and analogous to the behavior of other glasses such as SiO_2 , GeO_2 and GeS_2 [49–51]. As one can see from figure 6, pressure induced changes in the short range structural ordering in the g- GeSe_2 glass are similar under different experimental conditions (with or without Ne PTM), supporting what was observed from the XANES data. If there were significant amount of Ne penetration into voids and empty interstitial sites, the pressure behavior of g- GeSe_2 in the Ne pressure medium would be clearly different from the results obtained without PTM, as in case of the silica glass loaded together with He which show huge differences in the structure and compression behavior [8, 18, 52]. Moreover, presence of considerable amounts of Ne within the glass network would change both the XANES spectral profile and EXAFS signals, a Ne induced contribution would be visible in both Se and Ge K-edge data. Even if the possibility of a very minor diffusion of Ne cannot be excluded, results of the present high pressure XAS experiments confirms the absence of a significant Ne incorporation into the g- GeSe_2 glass within pressure ranges up to 45 GPa. Even though the effects of using Ne as PTM on the pressure behavior of glasses have to be verified for individual cases, our findings suggest that Ne can be used as PTM for high pressure EXAFS experiments at least for some glasses including g- GeSe_2 .

5. Conclusions

A detailed high-pressure x-ray absorption investigation of glassy GeSe_2 has been presented in this work. Experiments have been performed up to 45 GPa under different conditions, without using PTM and using Ne as pressure medium. The observed edge shifts at the Se and Ge K-edges for increasing pressures allowed us to identify the metallization onsets by direct observation of a 1.5 eV red-shift at the Ge K-edge, which occur smoothly in the 10–20 GPa range. The semiconductor–metal transition was thus observed to happen gradually within the 10–20 GPa, forming a stable metallic form above 20 GPa.

We also performed accurate double-edge EXAFS refinements using advanced data-analysis methods (GNXAS) to evaluate the pressure induced modifications of the first-neighbor distribution. The observed trend in the structural parameters is characterized by three stages of compression: (1) a first stage up to about 11 GPa in which the tetrahedral coordination around Ge atoms is substantially preserved; (2) a transition stage between 11 and 30 GPa in which we observed an elongation of the first-neighbor distances and an increase of coordination from 4 to about 5; (3) a third stage in which

the local structure is substantially stable with a slight increase in coordination.

Our EXAFS analysis added useful information to the edge-shift determination and showed that the transition from tetrahedral to octahedral coordination around Ge sites is not fully achieved even at 45 GPa. Present experiments also show that the structural behavior of g-GeSe₂ under pressure is not noticeably affected by the presence of Ne PTM, confirming the absence of a significant Ne incorporation into the GeSe₂ glass within pressure range up to 45 GPa.

Data availability statement

All data that support the findings of this study are included within the article (and any supplementary files).

Acknowledgments

We acknowledge the European Synchrotron Radiation Facility (ESRF) for provision of synchrotron radiation facilities (Proposal No: HC-4645). We would like to warmly thank J Jacobs for his help with the preparation and gas loading of the diamond anvil cells. E M thanks for the ‘GO FOR IT’ postdoc grant from the CRUI (Conferenza dei Rettori delle Università Italiane) foundation.

ORCID iDs

Emin Mijit  <https://orcid.org/0000-0002-9232-2538>

João Elias F S Rodrigues  <https://orcid.org/0000-0002-9220-5809>

Francesco Paparoni  <https://orcid.org/0000-0002-8210-7586>

References

- [1] Daisenberger D, Wilson M, McMillan P F, Cabrera R Q, Wilding M C and Machon D 2007 *Phys. Rev. B* **75** 224118
- [2] Di Cicco A, Congeduti A, Coppari F, Chervin J C, Baudelet F and Polian A 2008 *Phys. Rev. B* **78** 033309
- [3] Prescher C, Prakapenka V B, Stefanski J, Jahn S, Skinner L B and Wang Y 2017 *Proc. Natl Acad. Sci.* **114** 10041–6
- [4] Itie J P, Polian A, Calas G, Petiau J, Fontaine A and Tolentino H 1989 *Phys. Rev. Lett.* **63** 398–401
- [5] Mishima O, Calvert L and Whalley E 1985 *Nature* **314** 76–78
- [6] Sato T and Funamori N 2008 *Phys. Rev. Lett.* **101** 255502
- [7] Coppari F, Chervin J, Congeduti A, Lazzeri M, Polian A, Principi E and Di Cicco A 2009 *Phys. Rev. B* **80** 115213
- [8] Shen G, Mei Q, Prakapenka V B, Lazor P, Sinogeikin S, Meng Y and Park C 2011 *Proc. Natl Acad. Sci.* **108** 6004–7
- [9] Murakami M and Bass J D 2010 *Phys. Rev. Lett.* **104** 025504
- [10] Sato T, Funamori N and Yagi T 2011 *Nat. Commun.* **2** 1–5
- [11] Properzi L, Di Cicco A, Nataf L, Baudelet F and Irifune T 2015 *Sci. Rep.* **5** 10188
- [12] Properzi L, Santoro M, Minicucci M, Iesari F, Ciambezi M, Nataf L, Le Godec Y, Irifune T, Baudelet F and Di Cicco A 2016 *Phys. Rev. B* **93** 214205
- [13] Shelby J 1976 *J. Appl. Phys.* **47** 135–9
- [14] Roselieb K, Rammensee W, Büttner H and Rosenhauer M 1992 *Chem. Geol.* **96** 241–66
- [15] Clark A N, Leshner C E, Jacobsen S D and Wang Y 2016 *J. Geophys. Res.: Solid Earth* **121** 4232–48
- [16] Rosa A, Bouhifd M A, Morard G, Briggs R, Garbarino G, Irifune T, Mathon O and Pascarelli S 2020 *Earth Planet. Sci. Lett.* **532** 116032
- [17] Yang H, Gleason A E, Tkachev S N, Chen B, Jeanloz R and Mao W L 2021 *Geochem. Perspect. Lett.* **17** 1–5
- [18] Weigel C, Polian A, Kint M, Ruffe B, Foret M and Vacher R 2012 *Phys. Rev. Lett.* **109** 245504
- [19] Krstulović M, Rosa A D, Sanchez D F, Libon L, Albers C, Merkulova M, Grolimund D, Irifune T and Wilke M 2022 *Phys. Earth Planet. Inter.* **323** 106823
- [20] Klotz S, Chervin J, Munsch P and Le Marchand G 2009 *J. Phys. D: Appl. Phys.* **42** 075413
- [21] Di Cicco A 2020 *Radiat. Phys. Chem.* **175** 108077
- [22] Hong X, Newville M, Duffy T S, Sutton S R and Rivers M L 2013 *J. Phys.: Condens. Matter* **26** 035104
- [23] Krstulović M, Rosa A D, Biedermann N, Spiekermann G, Irifune T, Mu noz M and Wilke M 2020 *Phys. Rev. B* **101** 214103
- [24] Krstulović M, Rosa A D, Biedermann N, Irifune T and Wilke M 2021 *Chem. Geol.* **560** 119980
- [25] Bowron D T, Filipponi A, Roberts M A and Finney J L 1998 *Phys. Rev. Lett.* **81** 4164–7
- [26] Pohlentz J, Rosa A, Mathon O, Pascarelli S, Belin S, Landrot G, Murzin V, Veligzhanin A, Shiryayev A and Irifune T 2018 *Chem. Geol.* **486** 1–15
- [27] Irifune T, Kurio A, Sakamoto S, Inoue T and Sumiya H 2003 *Nature* **421** 599
- [28] Ishimatsu N, Matsumoto K, Maruyama H, Kawamura N, Mizumaki M, Sumiya H and Irifune T 2012 *J. Synchrotron Radiat.* **19** 768–72
- [29] Durandurdu M and Drabold D A 2002 *Phys. Rev. B* **65** 104208
- [30] Mei Q et al 2006 *Phys. Rev. B* **74** 014203
- [31] Wezka K et al 2014 *Phys. Rev. B* **90** 054206
- [32] Antao S M, Benmore C J, Li B, Wang L, Bychkov E and Parise J B 2008 *Phys. Rev. Lett.* **100** 115501
- [33] Properzi L, Di Cicco A, Nataf L, Baudelet F and Irifune T 2015 *Sci. Rep.* **5** 1–9
- [34] Dewaele A, Loubeyre P and Mezouar M 2004 *Phys. Rev. B* **70** 094112
- [35] Mathon O, Beteva A, Borrel J, Bugnazet D, Gatla S, Hino R, Kantor I, Mairs T, Munoz M and Pasternak S et al 2015 *J. Synchrotron Radiat.* **22** 1548–54
- [36] Wu Z Y, Gota S, Jollet F, Pollak M, Gautier-Soyer M and Natoli C R 1997 *Phys. Rev. B* **55** 2570–7
- [37] Mayer S F, Rodrigues J E, Marini C, Fernández-Díaz M, Falcón H, Asensio M C and Alonso J 2020 *Sci. Rep.* **10** 1–14
- [38] Mijit E, Chen K, Choueikani F, Di Cicco A and Baudelet F 2018 *Phys. Rev. B* **98** 184423
- [39] Mijit E, Chen K, Rodrigues J E F, Hu Z, Nataf L, Trapananti A, Di Cicco A and Baudelet F 2021 *Phys. Rev. B* **103** 024105
- [40] Chen K, Baudelet F, Mijiti Y, Nataf L, Di Cicco A, Hu Z, Agrestini S, Komarek A, Sougrati M and Haines J et al 2019 *J. Phys. Chem. C* **123** 21114–9
- [41] Mijiti Y, Perri M, Coquet J, Nataf L, Minicucci M, Trapananti A, Irifune T, Baudelet F and Di Cicco A 2020 A new internally heated diamond anvil cell system for time-resolved optical and x-ray measurements *Rev. Sci. Instrum.* **91** 085114
- [42] Chen K, Mijiti Y, Agrestini S, Liao S, Li X, Zhou J, Di Cicco A, Baudelet F, Tjeng L Hao and Hu Z 2018 Valence State of Pb in Transition Metal Perovskites PbTMO 3 (TM = Ti, Ni) Determined From X-Ray Absorption Near-Edge Spectroscopy *Phys. Status Solidi b* **255** 1800014

- [43] Rezvani S *et al* 2020 Structure rearrangements induced by lithium insertion in metal alloying oxide mixed spinel structure studied by x-ray absorption near-edge spectroscopy *J. Phys. Chem. Solids* **136** 109172
- [44] Mijit E, Trapananti A, Nataf L, Baudelet F, Shinmei T, Irifune T, Jiang J Z and Di Cicco A 2022 *Phys. Status Solidi* **16** 2100423
- [45] Filipponi A, Di Cicco A and Natoli C R 1995 *Phys. Rev. B* **52** 15122–34
- [46] Filipponi A and Di Cicco A 1995 *Phys. Rev. B* **52** 15135
- [47] Filipponi A and Di Cicco A 2000 *TASK Quart.* **4** 575–669
- [48] Di Cicco A 1996 *Phys. Rev. B* **53** 6174–85
- [49] Kono Y, Kenney-Benson C, Ikuta D, Shibazaki Y, Wang Y and Shen G 2016 *Proc. Natl Acad. Sci.* **113** 3436–41
- [50] Kono Y, Shu Y, Kenney-Benson C, Wang Y and Shen G 2020 *Phys. Rev. Lett.* **125** 205701
- [51] Vaccari M, Garbarino G, Aquilanti G, Coulet M-V, Trapananti A, Pascarelli S, Hanfland M, Stavrou E and Raptis C 2010 *Phys. Rev. B* **81** 014205
- [52] Sato T and Funamori N 2010 *Phys. Rev. B* **82** 184102